

Phenomenological analysis of tetragonal tungsten bronze ferroelectrics

L. E. CROSS

Materials Research Laboratory, The Pennsylvania State University, University Park, Pennsylvania 16802, USA

R. R. NEURGAONKAR

Rockwell Science Center, Thousand Oaks, California 91360, USA

A simple Devonshire form has been derived for the phenomenological elastic Gibbs function to describe the elasto-dielectric parameters of simple proper ferroelectrics in the tungsten bronze structure family which has 4/mmm prototypic point symmetry. For the assumption that all temperature dependence is carried by the Curie–Weiss behaviour implicit in the quadratic term and that the expansion may be terminated at the first sixth-order term, reasonable agreement between calculated and derived P_s against T curves in the ferroelectric phase can be obtained for a wide range of bronze compositions. From the fitting it is clear that second and sixth rank terms are remarkably constant over a very wide range of bronze compositions. Variation in the negative fourth rank term is larger, but this is to be expected since it contains large contributions from electrostrictive and elastic terms which will depend on boundary conditions. These initial studies suggest that the phenomenological method may be used to derive expectation values for tensor parameters across the whole family of ferroelectric bronzes. The study also points up the need for more careful detailed studies of lattice strain, birefringence and permittivity as a function of temperature in model bronze compounds to provide more detailed checks of the method.

1. Introduction

The tungsten bronze family of simple proper ferroelectrics incorporates now almost 100 different end member compositions, most of which are mutually compatible in solid solution, so that an immense range of possible ferroelectrics is available. In attempting to select compositions for device application in electro-optics, pyroelectric acousto-optics, surface acoustic wave (SAW), etc. it is important for each device to maximize a different combination of the tensor properties of the crystal, so that some theoretical predictive capability would be of major help in making rational choices in this bewildering range of possible bronze compositions. For complex structures like the ferroelectric bronzes, however, where different cations can have different fractional occupancy on several sites in the structure, a rigorous atomistic theory is at present out of the question. It is the purpose of this paper to explore the extent to which thermodynamic phenomenological methods can be used to correlate the tensor properties to point up the inadequacies of present experimental data and to suggest a more systematic experimental approach.

A rather simple Landau–Ginsburgh–Devonshire function for the elastic Gibbs free energy of simple proper ferroelectric bronzes which can be derived for the 4/mmm prototype symmetry has been discussed earlier [1], and the function was used with good results to fit the dielectric, electric and piezoelectric

properties of the $\text{Ba}_{0.40}\text{Sr}_{0.60}\text{Nb}_2\text{O}_6$ (SBN) ferroelectric composition [2]. A simple power series expansion up to the first sixth-power terms in polarization but including only fourth rank terms in elastic and elasto-electric coupling terms proved adequate to explain dielectric, piezoelectric and spontaneous shape change data; however it was necessary to include sixth order electrostriction to model the elastic constant behaviour. The relaxor dielectric character of SBN was taken into account by using a narrow distribution of Curie temperatures, T_C , and did not obtrude in the fitting process except for properties very close to \bar{T}_C where fluctuations in the polarization take \bar{P}_3^2 far from zero [3].

2. Thermodynamic phenomenology

Recapitulating our earlier studies, it has been the contention that an empirical thermodynamic elastic Gibbs function can be developed which will describe the polarization induced changes in the dielectric, elastic, thermal, piezoelectric and electro-optic properties in all possible simple proper ferroelectric phases of the tungsten bronze structure ferroelectrics.

Under the symmetry constraints of the 4/mmm point symmetry of the prototypic form of the bronzes, the permitted dielectric stiffnesses α_{ij} , fourth order stiffnesses α_{ijkl} , electrostriction constants Q_{ijkl} , elastic

compliances s_{ijkl} and sixth order dielectric stiffnesses α_{ijklmn} are listed in Tables I to IV.

Using the reduced notation 11 \rightarrow 1, 22 \rightarrow 2, 33 \rightarrow 3, 23 or 32 \rightarrow 4, 13 or 31 \rightarrow 5 and 12 or 21 \rightarrow 6, the elastic Gibbs function takes the form

$$\begin{aligned} \Delta G_1 = & \alpha_1(P_1^2 + P_2^2) + \alpha_3 P_3^2 + \alpha_{11}(P_1^4 + P_2^4) \\ & + \alpha_{33} P_3^4 + \alpha_{13}(P_1^2 P_3^2 + P_2^2 P_3^2) \\ & + \alpha_{12} P_1^2 P_2^2 + \alpha_{333} P_3^6 + \alpha_{111}(P_1^6 + P_2^6) \\ & - \frac{1}{2} s_{11}(X_1^2 + X_2^2) - s_{12} X_1 X_2 \\ & - s_{13}(X_1 + X_2) X_3 - \frac{1}{2} s_{33} X_3^2 \\ & - \frac{1}{2} s_{44}(X_4^2 + X_5^2) - \frac{1}{2} s_{66} S_6^2 \\ & - Q_{11}(P_1^2 X_1 + P_2^2 X_2) \\ & - Q_{12}(P_1^2 X_2 + P_2^2 X_1) \\ & - Q_{13}(P_1^2 X_3 + P_2^2 X_3) \\ & - Q_{31}(P_3^2 X_1 + P_3^2 X_2) - Q_{33} P_3^2 X_3 \end{aligned}$$

$$\begin{aligned} & - Q_{44}(P_2 P_3 X_4 + P_1 P_3 X_5) \\ & - Q_{66} P_1 P_2 X_6 \end{aligned} \quad (1)$$

The first partial derivatives with respect to the polarization give the field components

$$\begin{aligned} \frac{\partial \Delta G}{\partial P_1} = E_1 = & 2\alpha_1 P_1 + 4\alpha_{11} P_1^3 + 2\alpha_{13} P_1 P_3^2 \\ & + 2\alpha_{12} P_1 P_2^2 + 6\alpha_{111} P_1^5 \\ & + Q_{13} P_1 X_3 + Q_{44} P_3 X_5 \\ & + Q_{66} P_1 X_6 \end{aligned} \quad (2)$$

$$\begin{aligned} \frac{\partial \Delta G}{\partial P_2} = E_2 = & 2\alpha_1 P_2 + 4\alpha_{11} P_2^3 + 2\alpha_{13} P_2 P_3^2 \\ & + 2\alpha_{12} P_2 P_1^2 + 6\alpha_{111} P_2^5 \\ & + 2Q_{13} P_2 X_3 + Q_{44} P_3 X_4 \\ & + Q_{66} P_1 X_6 \end{aligned} \quad (3)$$

TABLE I Equivalent second and fourth rank dielectric terms for 4/mmm symmetry

Nye's matrix notation		Full tensor notation		Number of equivalent terms
Term	Symmetry equivalent terms	Term	Symmetry equivalent terms	
α_1	α_2	α_{11}	α_{22}	2
α_3		α_{33}		1
α_{11}	α_{22}	α_{1111}	α_{2222}	2
α_{12}	α_{21}, α_{66}	α_{1122}	$\alpha_{1212}, \alpha_{1221}, \alpha_{2112}, \alpha_{2121}, \alpha_{2211}$	12
α_{13}	$\alpha_{31}, \alpha_{23}, \alpha_{32}, \alpha_{44}, \alpha_{55}$ ($\alpha_{44} = 4\alpha_{2323}$)	α_{1133}	$\alpha_{3311}, \alpha_{2233}, \alpha_{1313}, \alpha_{1313}, \alpha_{1331}, \alpha_{3113},$ $\alpha_{3131}, \alpha_{2323}, \alpha_{2332}, \alpha_{3223}, \alpha_{3232}$	1
α_{33}		α_{3333}		1

TABLE II Equivalent electrostriction terms for 4/mmm symmetry

Nye's matrix notation		Full tensor notation		Number of equivalent terms
Term	Symmetry equivalent terms	Term	Symmetry equivalent terms	
Q_{11}	Q_{22}	Q_{1111}	Q_{2222}	2
Q_{12}	Q_{21}	Q_{1122}	Q_{2211}	2
Q_{13}	Q_{23}	Q_{1133}	Q_{2233}	2
Q_{31}	Q_{32}	Q_{3311}	Q_{3322}	2
Q_{33}		Q_{3333}		1
Q_{44}	Q_{45}	Q_{2323}	$Q_{2332}, Q_{3223}, Q_{3232}, Q_{1313}, Q_{1331},$ Q_{8113}, Q_{3151}	8
Q_{66}		Q_{1212}	$Q_{1221}, Q_{2112}, Q_{2121}$	4

TABLE III Equivalent elastic compliance terms for 4/mmm symmetry

Nye's matrix notation		Full tensor notation		Number of equivalent terms
Term	Symmetry equivalent terms	Term	Symmetry equivalent terms	
s_{11}	s_{22}	s_{1111}	s_{2222}	2
s_{12}	s_{21}	s_{1122}	s_{2211}	2
s_{13}	s_{11}, s_{23}, s_{32}	s_{1133}	$s_{3311}, s_{2233}, s_{3322}$	4
s_{33}		s_{3333}		1
s_{44}	s_{55}	s_{2323}	$s_{2332}, s_{3223}, s_{3232}, s_{1313}, s_{1331},$ s_{3113}, s_{3131}	8
s_{66}		s_{1212}	$s_{1221}, s_{2112}, s_{2121}$	4

TABLE IV Equivalent sixth rank tensor terms of the form $\alpha(P^6)$ for 4/mmm symmetry

Term	Symmetry related terms	Number of equivalent terms
1. α_{111}	222	2
2. α_{112}	166, 121, 616, 661, 211, 221, 266, 212, 626, 662, 122	30
3. α_{113}	155, 131, 515, 551, 331, 223, 244, 232, 424, 442, 322	30
4. α_{123}	144, 132, 525, 645, 546, 636, 663, 564, 654, 552, 321, 441, 231, 465, 366, 255, 456, 213, 414, 312	90
5. α_{133}	535, 553, 331, 355, 313, 233, 434, 443, 332, 344, 323	30
6. α_{333}		1

$$\frac{\partial \Delta G}{\partial P_3} = E_3 = 2\alpha_3 P_3 + 4\alpha_{33} P_3^3 + 2\alpha_{13}(P_1^2 + P_2^2)P_3 + 6\alpha_{33} P_3^5 + 2Q_{31} P_3 (X_1 + X_2) + 2Q_{33} P_3 X_3 + Q_{44}(P_2 X_4 + P_1 X_5) \quad (4)$$

It is the solutions of these equations with $E_i = 0$ which determine the ferroelectric states for a free crystal ($X = 0$). In general, there are seven possible ferroelectric species which can occur from the prototypic 4/mmm symmetry of the para-electric phase of the tungsten bronze, each of which corresponds to a different combination of non-zero (spontaneous) values of the P_i components. All possible solutions for the three Equations 2–4 were derived and reported by Cross and Pohanka [4]. Practically, however, just two of these solutions encompass all presently known simple ferroelectric bronzes. These are

$$(a) \quad P_3^2 \neq 0 \quad P_1 = P_2 = 0$$

$$(b) \quad P_1^2 = P_2^2 \neq 0 \quad P_3 = 0$$

The species (a) corresponds to the Shuvalov [5] species 4/mmm (1) D4 F4mm where 4/mmm is the high temperature prototype point group and F4mm means that the crystal is ferroelectric of point group 4mm below the transition temperature. D4 indicates that the spontaneous polarization P_s has definite orientation along the four-fold symmetry axes, and (1) denotes number of equivalent four-fold axes, which is one. In other words, there are two domains of opposite orientation of P_s (i.e., 180° domains) along the four-fold prototypic axis. The second species (b) is one of the subtypes of 4/mmm (2) D2 Fmm2 with P_s along the two-fold axis which make angles of 45° with 1 and 2 prototype axis ($P_1^2 = P_2^2$) and has four equivalent ferroelectric domain states.

Substituting condition a into the general Equations 2–4 gives the following conditions for stability:

$$P_1 = P_2 = 0 \quad 0 = 2\alpha_3 + 4\alpha_{33} P_3^2 + 6\alpha_{333} P_3^4 \quad (5)$$

The isothermal dielectric stiffnesses, χ_{ij} , are

$$\chi_{11}^T = 2\alpha_1 + 2\alpha_{13} P_3^2$$

$$\chi_{22}^T = 2\alpha_1 + 2\alpha_{13} P_3^2$$

$$\chi_{33}^T = 2\alpha_3 + 12\alpha_{33} P_3^2 + 30\alpha_{333} P_3^4$$

$$\chi_{12}^T = \chi_{13}^T = \chi_{23}^T = 0 \quad (6)$$

The tetragonal spontaneous strains are given by

$$x_1 = Q_{31} P_3^2$$

$$x_2 = Q_{31} P_3^2$$

$$x_3 = Q_{33} P_3^2$$

$$x_4 = x_5 + x_6 = 0 \quad (7)$$

and the piezoelectric b coefficients by

$$b_{11} = 0 \quad b_{21} = 0 \quad b_{31} = 2Q_{31} P_3$$

$$b_{12} = 0 \quad b_{22} = 0 \quad b_{32} = 2Q_{31} P_3$$

$$b_{13} = 0 \quad b_{23} = 0 \quad b_{33} = 2Q_{33} P_3$$

$$b_{14} = 0 \quad b_{24} = Q_{44} P_3 \quad b_{44} = 0$$

$$b_{15} = Q_{44} P_3 \quad b_{25} = 0 \quad b_{35} = 0$$

$$b_{16} = 0 \quad b_{26} = 0 \quad b_{36} = 0 \quad (8)$$

For the case of conditions b the corresponding equations take the form, for the stability conditions,

$$P_1^2 = P_2^2 \quad 0 = 2\alpha_1 + (4\alpha_{11} + 2\alpha_{12})P_1^2 + 6\alpha_{111} P_1^4$$

$$P_3 = 0 \quad (9)$$

Isothermal stiffnesses are

$$\chi_{11}^T = 2\alpha_1 + 12\alpha_{11} P_1^2 + 2\alpha_{12} P_1^2 + 30\alpha_{111} P_1^4$$

$$\chi_{22}^T = 2\alpha_1 + 12\alpha_{11} P_1^2 + 2\alpha_{12} P_1^2 + 30\alpha_{111} P_1^4$$

$$\chi_{33}^T = 2\alpha_3 + 4\alpha_{13} P_1^2$$

$$\chi_{34}^T = 4\alpha_{12} P_1^2 \quad \chi_{13} = \chi_{23} = 0 \quad (10)$$

It may be noted that the coefficients here are expressed with respect to the original prototypic axes and thus satisfy pseudomonoclinic symmetry. However, a simple rotation of the matrix by 45° in the 1,2 plane would reveal the true orthorhombic symmetry.

Spontaneous elastic strains take the form

$$x_1 = (Q_{11} + Q_{12})P_1^2$$

$$x_2 = (Q_{11} + Q_{12})P_1^2$$

$$x_3 = 2Q_{13} P_1^2$$

$$x_6 = Q_{66} P_1^2 \quad x_4 = x_5 = 0 \quad (11)$$

and the piezoelectric coefficients are

$$b_{11} = 2Q_{11} P_1 \quad b_{21} = 2Q_{12} P_1 \quad b_{31} = 0$$

$$b_{12} = 2Q_{12} P_1 \quad b_{22} = 2Q_{11} P_1 \quad b_{32} = 0$$

$$b_{13} = 2Q_{13} P_1 \quad b_{23} = 2Q_{13} P_1 \quad b_{33} = 0$$

$$b_{14} = 0 \quad b_{24} = 0 \quad b_{34} = Q_{44} P_1$$

$$b_{15} = 0 \quad b_{25} = 0 \quad b_{35} = Q_{44} P_1$$

$$b_{16} = Q_{66} P_1 \quad b_{26} = Q_{66} P_1 \quad b_{36} = 0 \quad (12)$$

3. Potential utility of the phenomenological theory

3.1. Introduction

It is evident from Tables I to IV that a substantial number of constants are required to characterize the

bronzes in this phenomenological manner. The only formal benefit is that all the elasto-dielectric parameters of the lower symmetry ferroelectric forms can be characterized in terms of the nonlinear parameters of the higher symmetry prototype form.

In principle, it is possible that all the parameters can be functions of both temperature and composition; however, several pieces of evidence, both direct and indirect, suggest that:

(a) The dominant temperature dependence is carried in the terms α_1 and α_3 which have a Curie-Weiss form

$$\begin{aligned}\alpha_1 &= \alpha_{10}(T - \theta_1) \\ \alpha_3 &= \alpha_{30}(T - \theta_3).\end{aligned}\quad (13)$$

(b) The higher order constants do not change markedly with either temperature or composition across a wide field of compounds and solid solutions with bronze structure.

In earlier studies we have demonstrated the following.

(i) In all known ferroelectric bronzes, only two of the seven possible ferroelectric species which are available from the 4/mmm prototype occur in nature.

(ii) In the tetragonal ferroelectric form in $(\text{Sr}_{0.61}\text{Ba}_{0.39})\text{Nb}_2\text{O}_6$ which is the congruently melting SBN composition, the data followed very closely to the phenomenology except for temperature close to the Curie point T_C and all parameters have been evaluated.

(iii) For the $(\text{Pb}_{1-x}\text{Ba}_x)\text{Nb}_2\text{O}_6$ compositions in the tetragonal phase field but close to the morphotropic phase boundary at the $(\text{Pb}_{0.6}\text{Ba}_{0.4})\text{Nb}_2\text{O}_6$ composition, the dielectric, piezoelectric and electrooptic behaviour can be quite accurately modelled using the phenomenological constants for SBN and just adjusting θ_1 and Q_3 to conform to the observed Curie-Weiss behaviour in these compositions [6].

The success to date with the modelling suggest that we attempt a more ambitious assessment of the range of validity of our simple hypotheses (a) and (b) using a much wider range of bronze compounds and making use of literature values to evaluate directly, wherever possible, the stiffness parameters. The results of this effort will form the bulk of this paper.

A second feature which has become evident from our modelling of the tungsten bronze ferroelectrics is that, particularly in the elastic response, the relaxor character of the bronzes is reflected in a breakdown of the static phenomenological model at temperatures close to T_C due to the onset of fluctuations in P . Thus for a range of temperatures above T_C it is evident that though $\bar{P} = 0$, it is rigorously true that $\bar{P}^2 \neq 0$. The onset of a substantial fluctuating component in P will clearly affect all parameters which depend on even powers of P such as the linear dimensions, since

$$x_{ij} = Q_{ij33}P_3^2 \quad (14)$$

the optical refractive index as

$$\Delta B_{ij} = g_{ij33}P_3^2 \quad (15)$$

and the elastic compliance

$$s_{ijkl} = \Phi_{ijkl33}P_3^2 \quad (16)$$

Perhaps the easiest to analyse is the strain response, and this will be the subject of a subsequent paper.

3.2. Evaluation of the thermodynamic parameters

In spite of the fact that more than 100 different ferroelectric compounds with the tungsten bronze structure have been synthesized, and innumerable solid solutions can be made between these end member compositions, there is a genuine paucity of reliable experimental data from which to evaluate the thermodynamic constants. For many materials, only ceramic samples have been made, and in these it is impossible to separate the individual tensor components. Even in many systems where good single crystals have been grown, the headlong rush to print has left many of the important parameters unmeasured.

For this study we have been able to find adequate but incomplete data for several $\text{Ba}_x\text{Sr}_{1-x}\text{Nb}_2\text{O}_6$ solid solutions. In several $\text{La}_2\text{O}_3:\text{KSr}_2\text{Nb}_5\text{O}_{15}$ compounds and solid solutions and for pure $\text{KSr}_2\text{Nb}_5\text{O}_{15}$ there is also adequate though incomplete data. $\text{NaNb}_2\text{Nb}_5\text{O}_{15}$ may be analysed on this model if the weak ferroelastic phase change near 370°C is neglected, and there is some data for a titanium modified $\text{NaNb}_2\text{Nb}_5\text{O}_{15}$. Similarly in $\text{K}_3\text{Li}_2\text{Nb}_5\text{O}_{15}$ there is adequate data for some of the constants though the transverse dielectric response has apparently not been measured.

In the orthorhombic ferroelectric form, we have only been able to find data for PbNb_2O_6 and for $\text{Pb}_2\text{KNb}_5\text{O}_{15}$. The fitting to obtain the thermodynamic parameters is, however, more difficult in these compositions and will be covered in a subsequent paper.

For the tetragonal ferroelectric form, the evaluation is relatively straightforward. The constant α_3 has the form $\alpha_3 = \alpha_{30}(T - \theta_3)$ which leads to an equation for the stiffness χ_{33} above T_C of the form

$$\chi_{33} = 2\alpha_{30}(T - \theta_3) \quad (17)$$

Thus the extrapolation of the Curie-Weiss plot of stiffness above T_C gives the temperature θ and the slope in the constant $2\alpha_{30}$.

By equating the ΔG values in ferroelectric and paraelectric states at T_C , the equation for P_s (5) can be put into the Devonshire form

$$\frac{T - \theta}{T_C - \theta} - 4\left(\frac{P_3}{P_{30}}\right)^2 + 3\left(\frac{P_3}{P_{30}}\right)^4 = 0 \quad (18)$$

in which $T_C - \theta$ and P_{30} are the only fitting parameters.

Often, unfortunately, the published P_s against T data for ferroelectric crystals is unreliable particularly at temperatures remote from T_C where it is often difficult to pole to a single domain state. Thus it is wise to check the shape of the polarization function by using a less direct method, e.g. the spontaneous strains $\Delta c/c$, $\Delta a/a$ induced in the ferroelectric form are electrostrictive in nature and thus scale with P_s^2 . Similarly the optical impermeability changes below

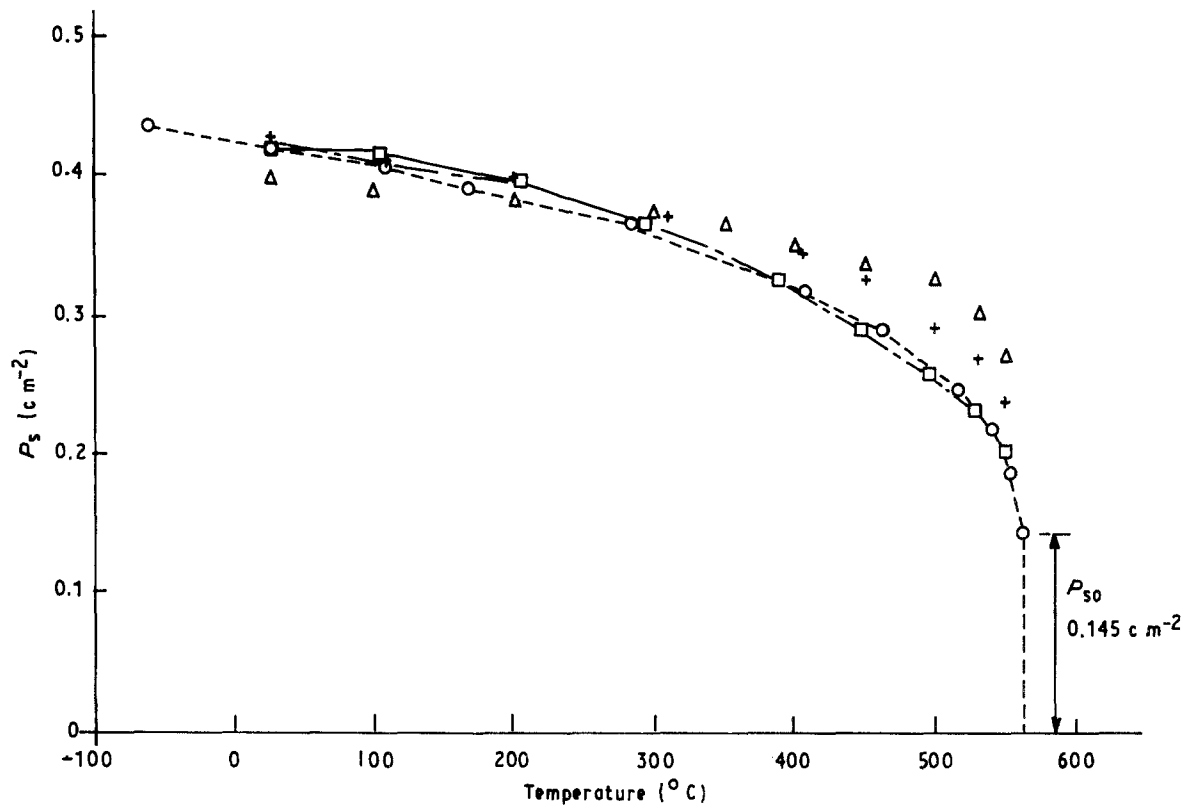


Figure 1 Phenomenological fitting of P_s against T in $\text{NaBa}_2\text{Nb}_5\text{O}_{15}$, show \circ , phenomenology; Δ , nonlinear optical results; +, pyroelectric measurement; \square , optical impermeability. $T_C = 563^\circ\text{C}$, $\theta_3 = 560^\circ\text{C}$, $P_{s0} = 0.145 \text{ c m}^{-2}$.

T_C (ΔB_{11} and ΔB_{33}) are again quadratic and scale with P_s^2 . Piezoelectric b_{ij} constants on the other hand, being morphic, scale directly with P_s , as does the linear electro-optic effect and the nonlinear Miller δ coefficients.

A typical fitting of the different P_s data for $\text{Ba}_2\text{NaNb}_2\text{O}_6$ is shown in Fig. 1. Clearly the Devonshire form is in excellent agreement with the "birefringence" data which are probably most reliable in this crystal. From the values of T_C , θ , P_{s0} and χ_{30} the α constants are given by

$$\alpha_3 = \frac{1}{2}\alpha_{30}(T_C - \theta_3) \quad (19)$$

$$\alpha_{33} = -\frac{\alpha_{30}(T_C - \theta_3)}{P_{s0}} \quad (20)$$

$$\alpha_{333} = \frac{\alpha_{30}(T_C - \theta_3)}{2(P_{s0})^4} \quad (21)$$

For the constants α_1 and α_{13} dielectric data for a section parallel to the c axis, ϵ_a , is required. Above T_C

$$\chi_1 = 2\alpha_{10}(T - \theta_1) \quad (22)$$

so that $2\alpha_{10}$ is the Curie-Weiss slope and θ_1 the extrapolated Curie temperature.

To derive α_{13} it is then a simple matter to make use of Equation 10 to obtain by least squares method a best fit to the experimental data below T_C , taking now calculated values for P_3 against T .

A typical plot comparing measured and calculated values for $\text{NaBa}_2\text{Nb}_5\text{O}_{15}$ is given in Fig. 2.

Using these methods constants for the bronze compositions derived are listed in Table V.

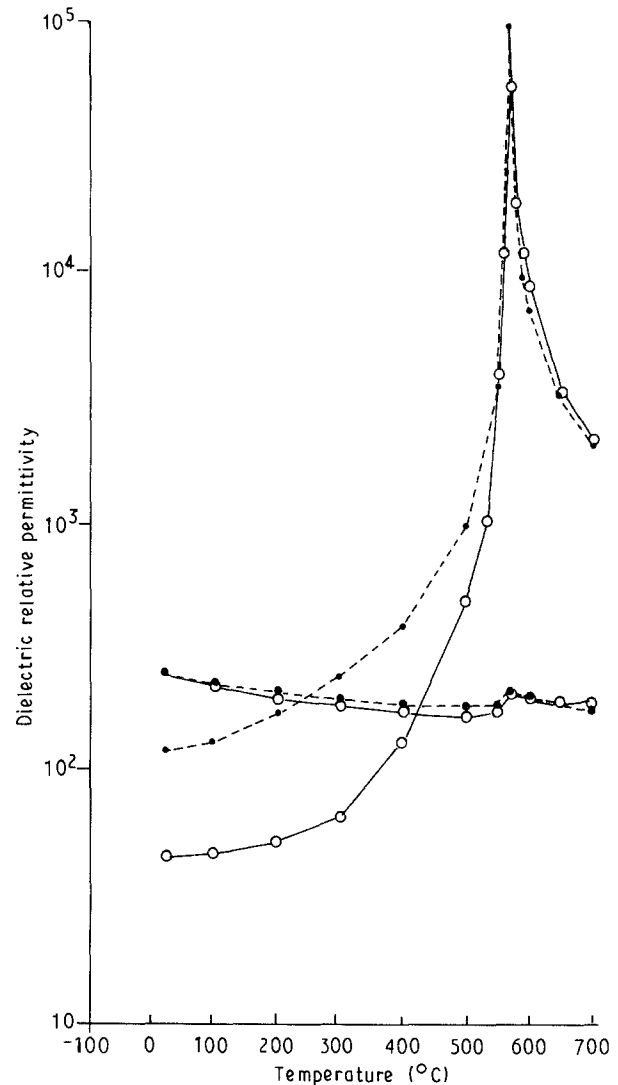


Figure 2 Phenomenological fitting to the dielectric permittivity in single crystal $\text{Ba}_2\text{NaNb}_5\text{O}_{15}$, showing (●●●) theory and (○ ○ ○) experiment.

3.3. Discussion

It may be noted at once that for α_{30} and α_{333} there is

TABLE V Thermodynamic constants for tetragonal tungsten bronze ferroelectric crystals

Compound	$\frac{1}{2}\alpha_{30}$	$12\alpha_{33}$	$30\alpha_{333}$	$\frac{1}{2}\alpha_{10}$	α_{13}
Ba _{0.75} Sr _{0.25} Nb ₂ O ₆	2.4×10^{-6}	-2.3×10^{-3}	3.6×10^{-1}		
Ba _{0.5} Sr _{0.5} Nb ₂ O ₆	2.4×10^{-6}	-6.2×10^{-3}	3.2×10^{-1}		
Ba _{0.4} Sr _{0.6} Nb ₂ O ₆	1.6×10^{-6}	-11.0×10^{-3}	3.6×10^{-1}		
Ba _{0.33} Sr _{0.67} Nb ₂ O ₆	2.7×10^{-6}	-1.6×10^{-3}	3.1×10^{-1}		
Ba _{0.39} Sr _{0.61} Nb ₂ O ₆	2.52×10^{-6}	-8.4×10^{-3}	3.6×10^{-1}	3.73×10^{-6}	2.1×10^{-3}
KSr ₂ Nb ₅ O ₁₅	3.45×10^{-6}	-9.7×10^{-3}	3.4×10^{-1}	2.4×10^{-6}	11.3×10^{-3}
3% (La) KSr ₂ Nb ₅ O ₁₅	2.2×10^{-6}	-9.6×10^{-3}	2.85×10^{-1}		
6% (La) KSr ₂ Nb ₅ O ₁₅	2.0×10^{-6}	-10.5×10^{-3}	3.8×10^{-1}		
9% (La) KSr ₂ Nb ₅ O ₁₅	3.14×10^{-6}	-12.2×10^{-3}	3.58×10^{-1}		
NaB ₂ Nb ₅ O ₁₅	3.44×10^{-6}	-11.46×10^{-3}	2.5×10^{-1}	5.15×10^{-6}	13.3×10^{-3}
Na _{1.65} Ba _{4.35} Nb _{9.65} Ti _{0.35} O ₃₀	3.56×10^{-6}	-5.34×10^{-3}	1.63×10^{-1}		
K ₃ Li ₂ Nb ₅ O ₁₅	2.87×10^{-6}	-14.16×10^{-3}	1.13×10^{-1}	2.82×10^{-6}	

excellent agreement over a very wide range of bronze compositions. The constant α_{10} is also within a narrow range, though here the stiffness is much larger and the Curie-Weiss slope more difficult to read precisely. The α_{33} values cover a wider range and this also is perhaps not surprising. In the elastic Gibbs function, the negative value of α_{33} comes about because of a strong contribution from elastic and electrostrictive constants in the free crystal. Thus the magnitude of α_{33} is markedly dependent on the elastic boundary conditions and probably therefore on the crystal perfection. The α_{13} values also cover a rather wider range, but here the error is probably in the evaluation.

In summary, it does appear from these preliminary data that the original hypothesis of a constancy of the higher order stiffnesses is a good approximation for the tetragonal bronze ferroelectrics, and thus can form a basis for the analysis of the properties of a very wide range of bronze compositions.

This research was jointly supported under the DARPA (N00014-82-C-2466) and ONR (N00014-81-C-0463) contracts.

References

1. L. E. CROSS, R. BETSCH, H. MCKINSTRY, T. SHROUT and R. R. NEURGAONKAR, in Proceedings of the 34th Frequency Control Symposium, May 1980 (IEEE).
2. T. R. SHROUT, L. E. CROSS, P. MOSES, H. A. MCKINSTRY and R. R. NEURGAONKAR, in Proceedings of the 1980 Ultrasonics Symposium, 1980, (IEEE) p. 414.
3. T. R. SHROUT, PhD thesis, The Pennsylvania State University (1981).
4. L. E. CROSS and R. C. POHANKA, *J. Appl. Phys.* **39** (1968) 3992.
5. L. A. SHUVALOV, *J. Phys. Soc. Suppl. (Jap.)* **28** (1970) 38.
6. T. R. SHROUT, D. A. HUKIN and L. E. CROSS, *Ferroelectric Lett.* **44** (1983) 325.

Received 25 November 1987
and accepted 3 March 1988